ISSN 2228-9860 eISSN 1906-9642 CODEN: ITJEA8

International Transaction Journal of Engineering, Management, & Applied Sciences & Technologies

http://TuEngr.com

Optimization of Low-Pressure Compressor Blades

M.L. Zhivirikhin[1], A.S. Tikhonov[1*]

[1] *Computer Engineering Center, FSBEI HE Peter the Great Saint Petersburg Polytechnic University, Saint-Petersburg, RUSSIA.*

**Corresponding Author (Email: Tikhonov@compmechlab.com).*

Paper ID: 12A10K

Volume 12 Issue 10

Received 05 May 2021
Received in revised form 24 July 2021
Accepted 28 July 2021
Available online 02 August 2021

Keywords:
Gas turbine engine; Low-pressure compressor; Blade profile; Parametric model; Gas-dynamic solver; Blade optimization; Head-capacity characteristic.

Abstract

In this article, the optimization of the low-pressure compressor blades is considered. The main research method was the joint use of the ANSYS CFX and IOSO PM software complexes. To improve the LPC characteristics, new models of blades with control of the midline curvature through the camber were developed, which improved the aerodynamics for supersonic flow modes. An original method of optimization problem decomposition is also proposed, which allows to significantly save the computing resources used. Optimization of the blades reduced the loss of kinetic energy and allowed to increase efficiency while preserving the performance parameters and dimensions of the LPC.

Disciplinary: Mechanical & Aerospace Engineering.

Cite This Article:

Zhivirikhin, M.L., Tikhonov, A.S. (2021). Optimization of Low-Pressure Compressor Blades. *International Transaction Journal of Engineering, Management, & Applied Sciences & Technologies, 12*(10), 12A10K, 1-15. http://TUENGR.COM/V12/12A10K.pdf DOI: 10.14456/ITJEMAST.2021.200

1 Introduction

When designing a gas turbine engine to reduce the cost of its life cycle, one of the most important factors is the compressor efficiency [1], which leads to the need to achieve high efficiency, performance, and the minimum possible compressor mass-dimensional parameters. Usually, this could be achieved with the growth of the compressor pressure ratio. However, it leads the engineers to challenge aerodynamic, strength, and vibration issues since the aerodynamic loading of the compressor stages also increases [2, 3]. For this reason, the first stages of the turbofan engines compressor often have vibration problems and, therefore, the shape of the rotor blades is commonly a compromise between high aerodynamic efficiency and reliability [3, 4, 5].

To achieve high efficiency of the compressor, it is necessary to suppress profile and wave losses in the blade rings, which leads to the development of increasingly complex working surfaces and a multiple increases in the complexity of the design process. At the same time, an increase in

the number of variables in parametric models has a contradictory effect on the parameters of the object under study.

To solve this problem successfully, the use of multi-criteria optimization methods is proposed based on the joint use of a gas-dynamic solver and an optimizer program as part of automated calculation chains. Based on such models, it is possible to automatically change the geometry of the compressor blades, which leads to an increase in efficiency while maintaining the design mode parameters. This can be traced in many publications [6–13] concerning the optimization of compressors, including using IOSO NM/PM, which allows increasing the efficiency of the compressor by 0.5...4% in the initial radial dimensions.

The purpose of this work is to increase the efficiency of the compressor by optimizing its blades while maintaining the performance parameters and mass-dimensional limitations.

In this work, a 4-stage low-pressure compressor (LPC) of the GTE for the drive of industrial equipment was studied, see Figure 1. This compressor has the following features:

- IGV controlled;
- anti-vibration shelves of the 1st and 2nd stages.

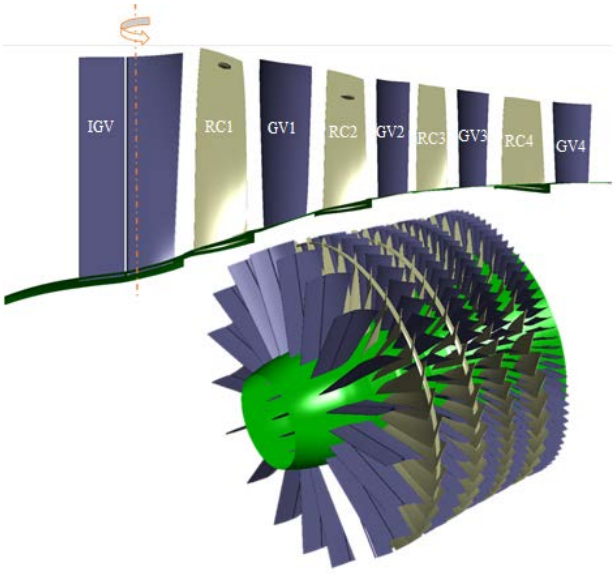

Figure 1: Original LPC

This compressor is a high-pressure one, in which the 1st (M = 0.7...1.15), 2nd (M = 0.78...0.92) and partially 3rd stages (M = 0.7...0.88) are trans- and supersonic blades.

2 Materials and Methods

In this work, a geometric scheme based on the variation of the cambers along the chord was used. This scheme was necessary for the implementation of the heterogeneous curvature of the profile based on the features of profiling supersonic blades.

The development of the blade parametric model implies the choice of a geometric scheme for forming a profile, as well as the definition of a set of variables and constants that characterize the blade profile.

During optimization, the parameters of the profile midline curvature were varied. The coordinates of the flow part contours, the distribution of thicknesses along with the profile, the relative position of the profiles in height compared to the original design did not change.

The geometry of the blade is described by the 3rd (stator blades) and 5th (rotor blades) equidistant sections (see figure2). The profile midline is determined by the 4th variables:

- Ga – profile installation angle,
- Ch – chord, mm;
- h1, h2, h3 – camber along the profile chord, mm.

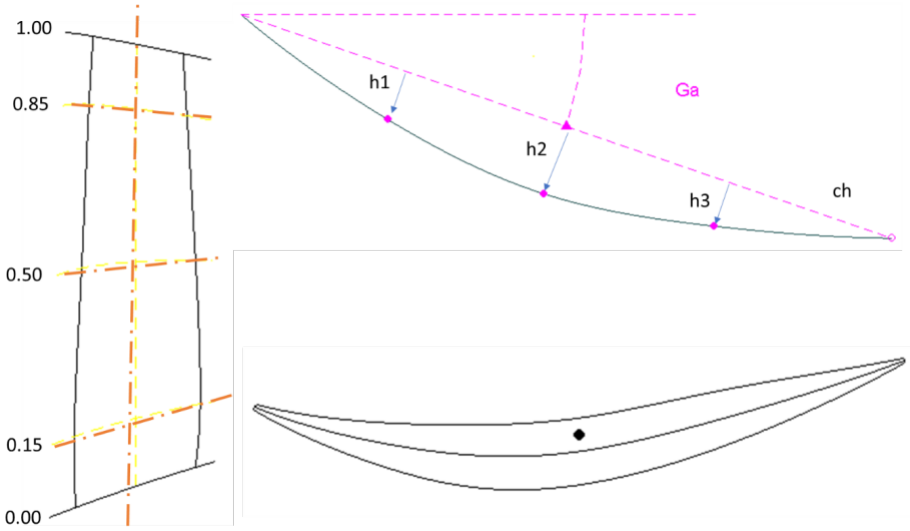

Figure2: Example of parameterization of RC1, profile at the bushing (h = 0%)

The total number of variables allocated for parameterization of the LPC blades is 114.

For the construction of finite element (FE) models, a block-structured grid builder [14] was used, a structured grid template based on a HEX element using the 4NO topology was used. The grids are constructed in a periodic formulation, the radial clearance on the blades is considered (see the example in Figure 3).

To perform the study, two options for configuring the FE model were used:

- simplified FE model with $Y^{+}C_c<5$, aspect ratio<2000 – for multicriteria optimization;
- detailed FE model with $Y^{+}C_c<2.5$, aspect ratio<2000 – for final calculated comparison.

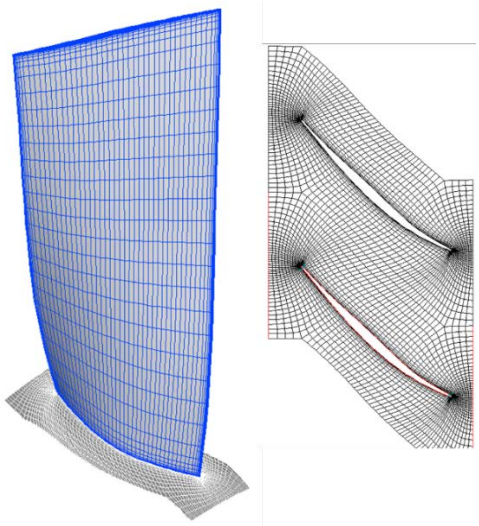

Figure 3: The example of RC1 FE model

To perform the viscous flow calculation in the compressor, the ANSYS CFX software package was used, the general view of the calculation model is shown in Figure 4. The main settings of the calculation model are given below:

- stationary (RANS) calculation [15];
- law of the total energy of heat exchange;
- k-ε [15-20] turbulence model;
- $1...7 \cdot 10^{-4}$ - physical time step;
- number of calculation iterations is 100...150;
- smooth walls of the blades and contours of the flow part without heat exchange;
- cyclic symmetry of the blade regions;
- stator-rotor interaction via "Stage" interfaces with speed averaging;
- ideal gas (air) is used as the working fluid, where μ, C_r, and λ depend on the temperature;

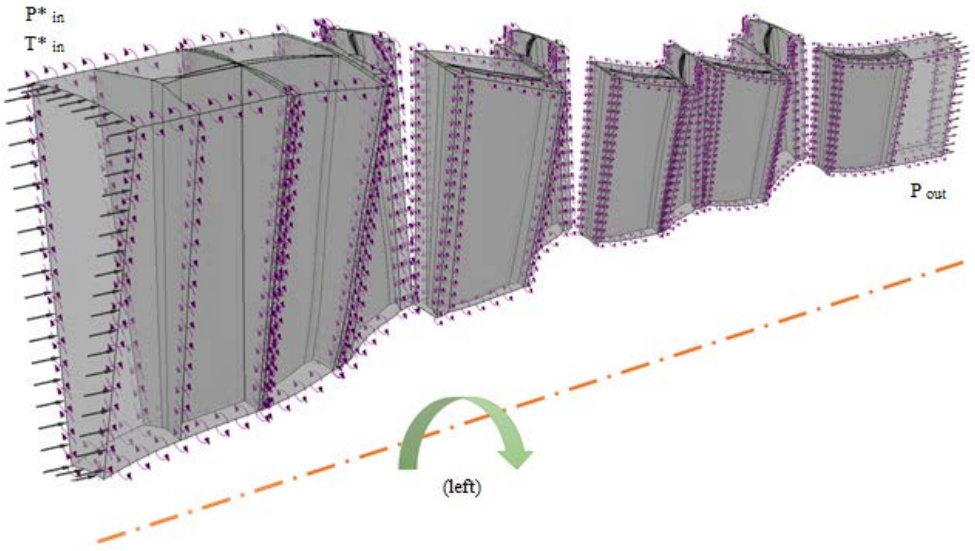

Figure 4: Calculation model of the LPC

The optimization process was divided into 3 stages:

- 1.5 stages;
- 2 stages;
- 2 stages.

Optimization was carried out in a given area with an overlap of 1 vane, the number of variable variables in one session did not exceed 50. The calculation area included the entire compressor (see figure5).

The LPC efficiency maximization ($\eta^*_k \uparrow$) was set as the objective function.

The following limitations were set:

- air consumption G_{in} ±0.5%;
- total pressure drop π^*_K ±0.05;
- residual twist angle α_2= ±3°;
- output speed $M_2 < 0.52$.

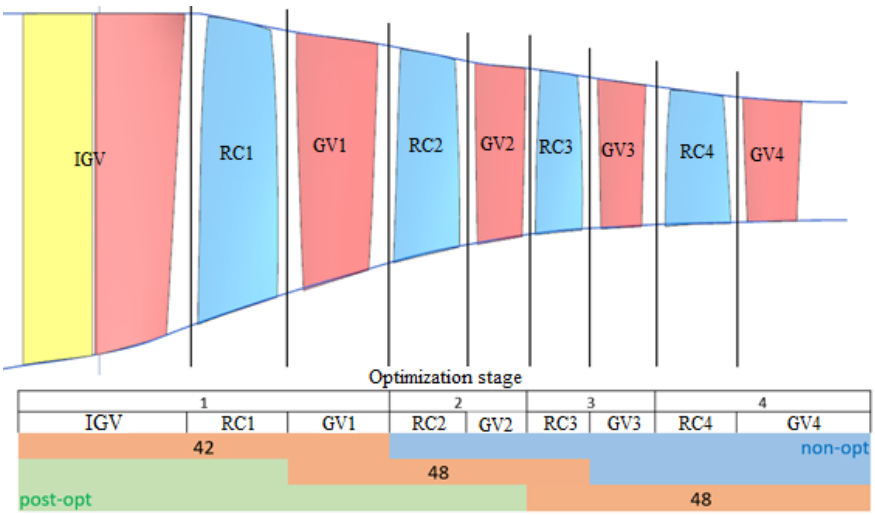

Figure 5: LPC decomposition diagram

3 Results and Discussions

After carrying out three optimization stages, new geometric models of the compressor blades were obtained, an increase in efficiency $\Delta\eta^*_k$ = +2.67% was achieved in the calculated mode.

IOSO PM demonstrated high efficiency of accumulative and heuristic procedures:

- after 200 requests, there is a significant increase in the density of obtaining successful solutions (see figure6);
- at all stages, the solution consists of 42...50 variables were found on average for 400 ... 500 requests to the mathematical model;
- a small number of non-calculated points.

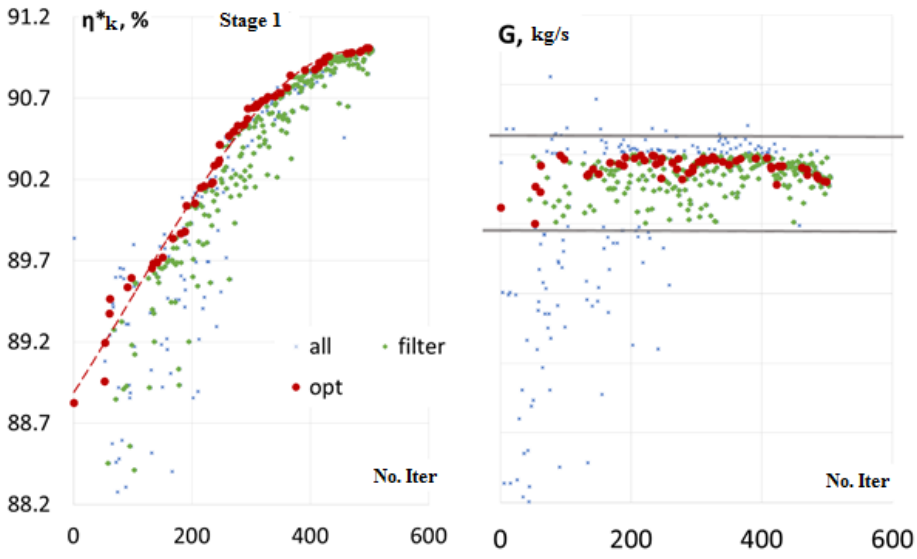

Figure 6: Dynamics of solution of the 1st stage optimization

The greatest increase in efficiency was achieved in RC1, a crown with a supersonic flow and a large elongation, due to the suppression of most parasitic effects. The main improvement was obtained by reducing the intensity of supersonic regions and shifting them to the channel depth - see Figures 7-10.

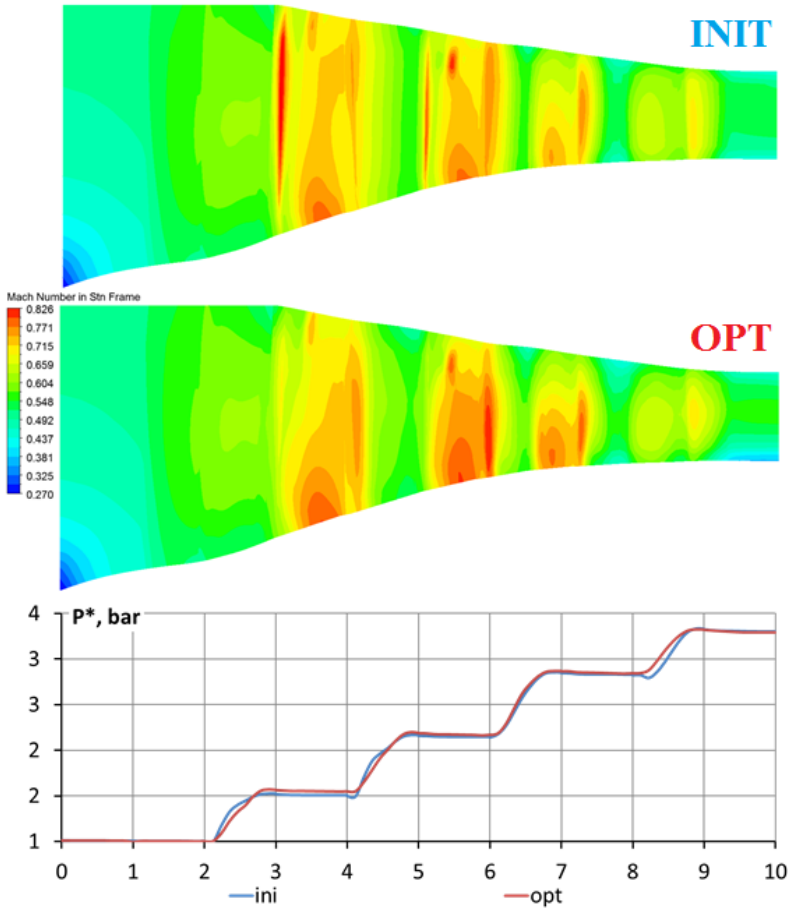

Figure 7: Distribution of the Mach number on the averaged meridional plane.

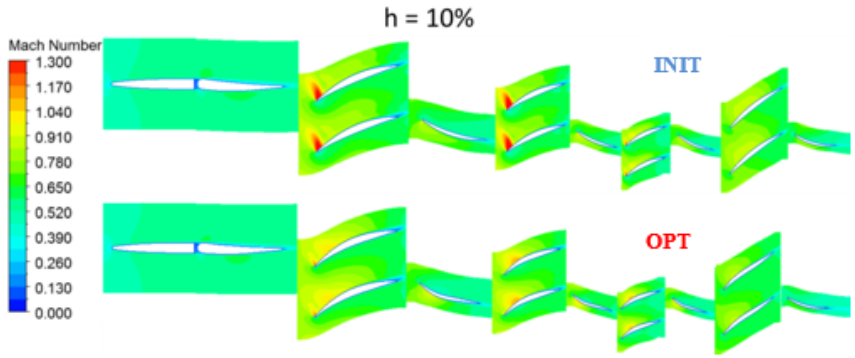

Figure 8: Mach number in the inter-blade channel at the bushing

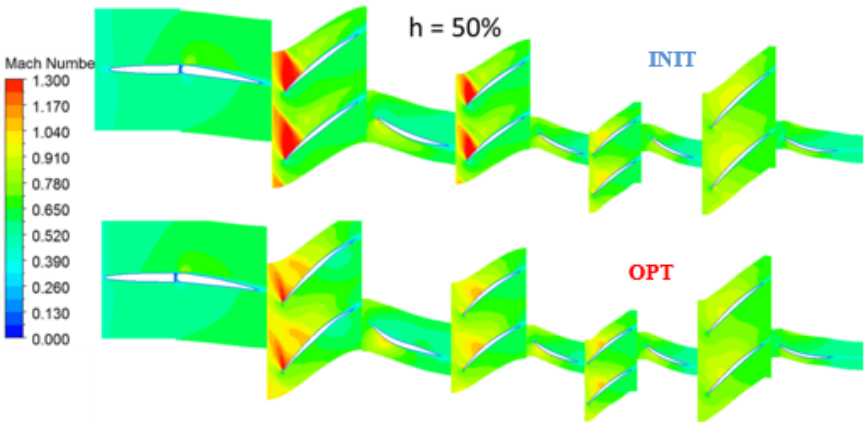

Figure 9: Mach number in the inter-blade channel at the average radius

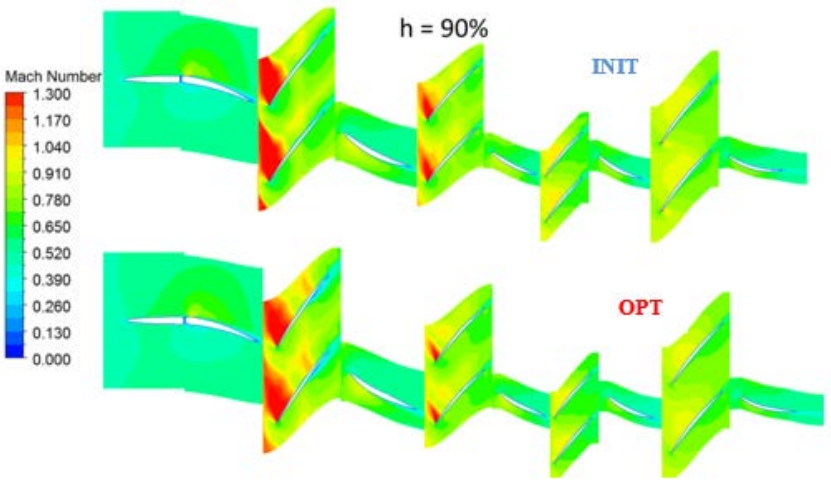

Figure 10: Mach number in the inter-blade channel at the periphery

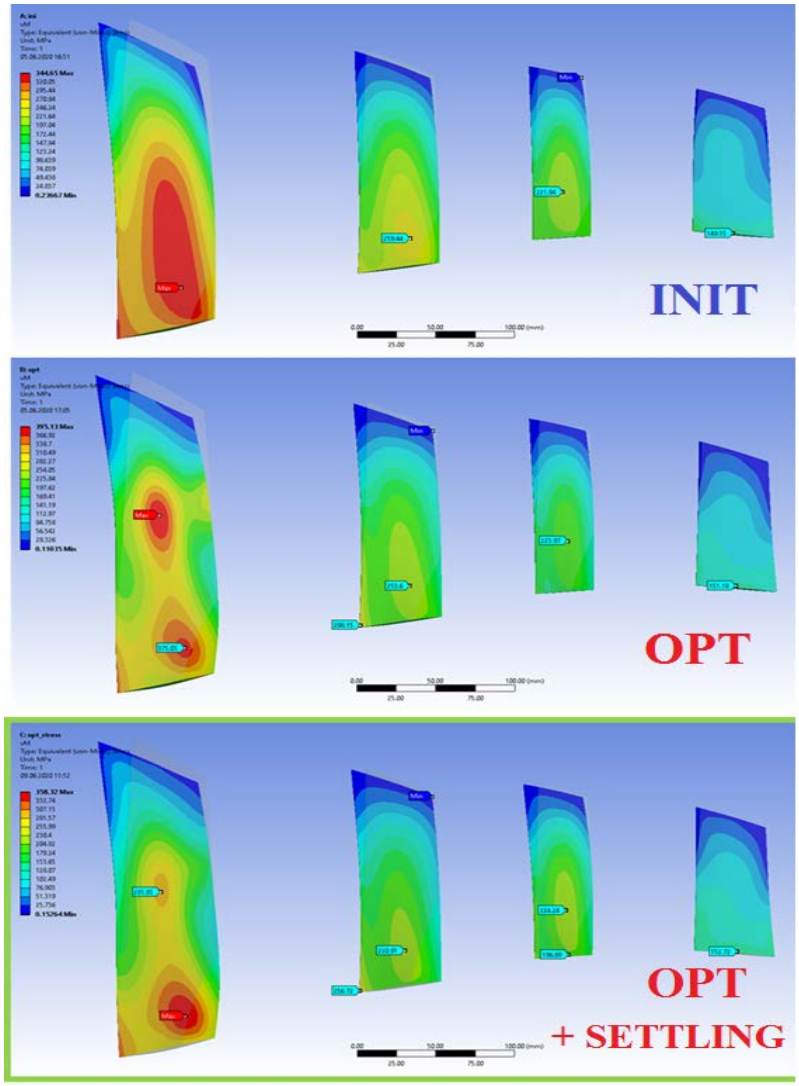

Figure 11: Comparison of equivalent stresses

Further, a preliminary comparative strength calculation of the initial and optimized compressor was carried out. The strength calculation was performed in the ANSYS workbench Static Structural software package. As boundary conditions, the following are applied to the blades: rotation speed, gas forces, and the average temperature at the maximum operating mode of

the engine. According to the calculation results of optimized blades, an increase in the equivalent stresses RC1 and RC2 by 15.5% and circumferential displacements by 7% is observed.

To prevent an increase in bending moments from gas forces, the bending gas force is compensated by centrifugal force by shifting the peripheral sections in the circumferential direction against rotation. The optimized compressor blades after compensation showed a significant reduction in stresses, the difference with the original version max 4% (Figure 11).

Then the final gas dynamic calculation of the pressure branches of the characteristic was carried out to compare the performance and efficiency in the operating modes of the original and optimized compressors:

- mod2 - original LPC;
- opt2 - optimized LPC.

As a result of the calculation of the characteristics, the following conclusions were obtained:

- for 0.8 and 0.9n branches, the optimization goals were achieved, the efficiency increase was $\Delta\eta_k^*$=+2...4%, the stability reserves were significantly increased;
- for the 0.95n branch, a decrease in the consumption of ΔG_v = - 3.5% and the efficiency of $\Delta\eta^*_k$ = -1% was obtained.

To ensure that the compressor optimization requirements were met, a local increase in the diameter of the RC1 periphery (by 7.5 mm, see Figure 12) was performed on the 0.95n pressure branch.

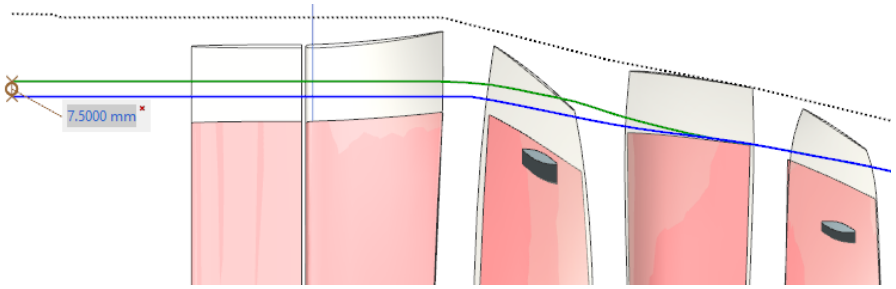

Figure 12: LPC model with a locally enlarged bypass RC1

Next, an additional calculation of the pressure branches of such LPC model is performed (indicated opt2+up, see Figure 13).

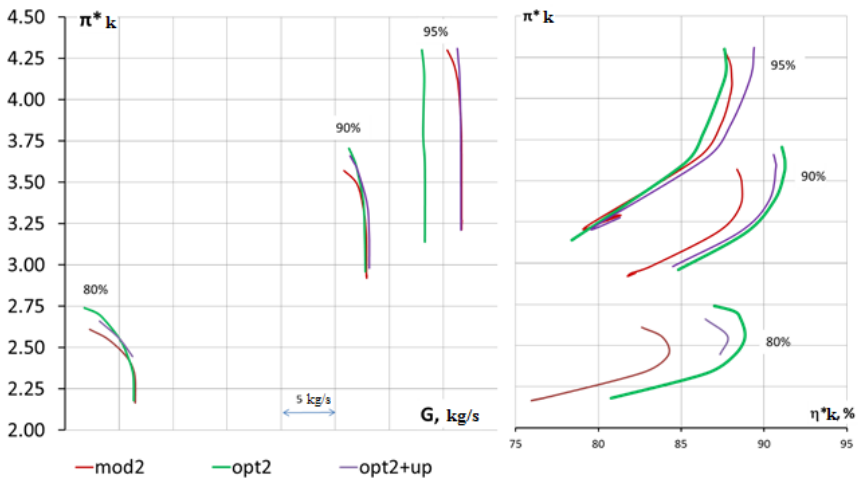

Figure 13: LPC characteristics

The calculation showed that the compressor optimization results are well scaled. It was possible to increase the throughput of the 1st stage with a slight loss of efficiency by local opening of the flow part (see Table 1).

Table 1: Comparison of the LPC parameters at the estimated calculation points

* n	Design option	π^*_k	n^*_k, %	$\Delta\eta^*_k$, %
0.7	mod2	2.44	84.23	-
	opt2	2.44	88.15	+3.92
	opt2+up	2.45	87.35	**+3.12**
0.9	mod2	3.34	88.54	-
	opt2	3.38	90.61	+2.07
	opt2+up	3.38	90.31	**+1.77**
0.95	mod2	3.84	87.39	-
	opt2	3.79	86.34	-1.05
	opt2+up	3.84	87.98	**+0.59**

Further, a detailed strength analysis of the developed structure was carried out. These models were created based on the Ansys workbench, using the second-order elements Solid 186 and Solid 187. The model of each RC includes a disk and a blade. When constructing the calculation models, the cyclic symmetry condition was applied. Thus, for the model of each RC, a sector with one blade was considered. Geometric models of the RC sectors are shown in Figure 14.

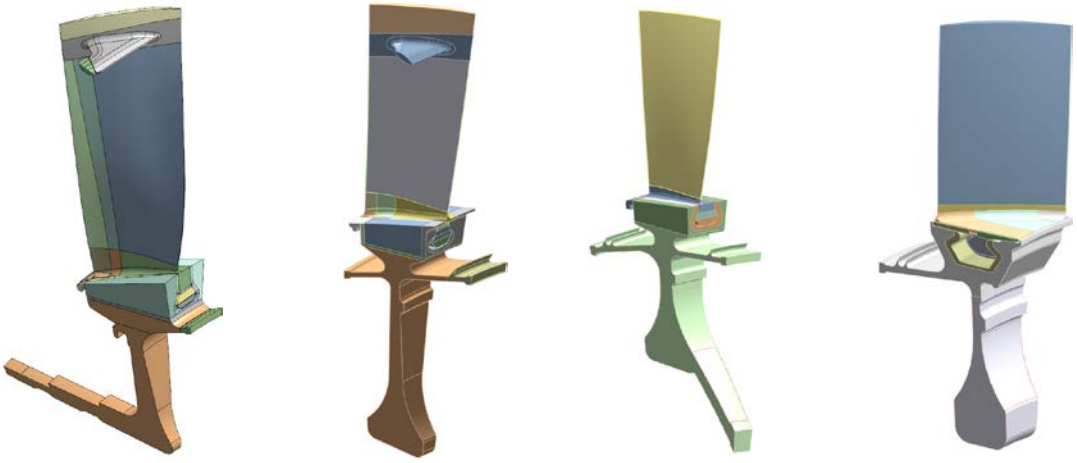

a) b) c) d)

a) - RC of the first stage; b) - RC of the second stage; c) - RC of the third stage; d) - RC of the fourth stage

Figure 14: Geometric models of the impeller sector

The following loads were considered:

- temperature (evenly distributed over the disk and blade of each RC);
- inertial load from rotation.

The contacts in the blade locks were created on the mating surfaces of the blade and disk, considering friction. The friction coefficient was taken to be 0.3. Fixing of the blade in the axial direction (for the first three RCs) was carried out by creating coupling equations between the nodes of the disk and the blade at the landing site of the locking ring.

The contact on the shroud was accepted as rigid linear (option bonded). Figure 15 shows the separation of the shroud geometry in the model to ensure contact under conditions of cyclic

symmetry. To ensure good convergence of the solution, and to obtain smooth gradients of the stress distribution in the contact zones of the locks, Solid 186 hexahedral FE was created. The size of the element was 0.5 mm. In places with irregular geometry in the contact zones, a size of 0.3 mm was accepted for the tetrahedral elements Solid 187. Figure 16 shows the grid quality in the locks.

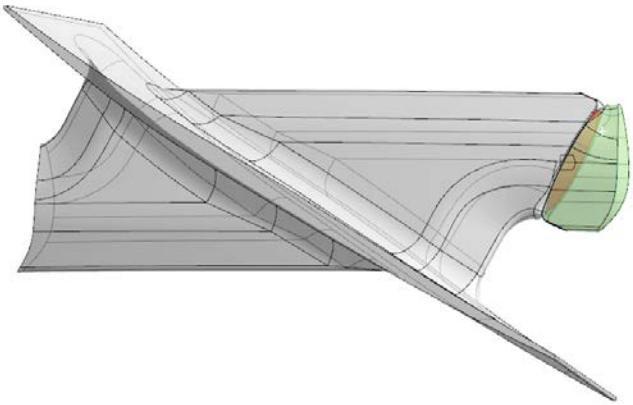

Figure 15: Separation of shroud geometry in the model to ensure contact in conditions of cyclic symmetry

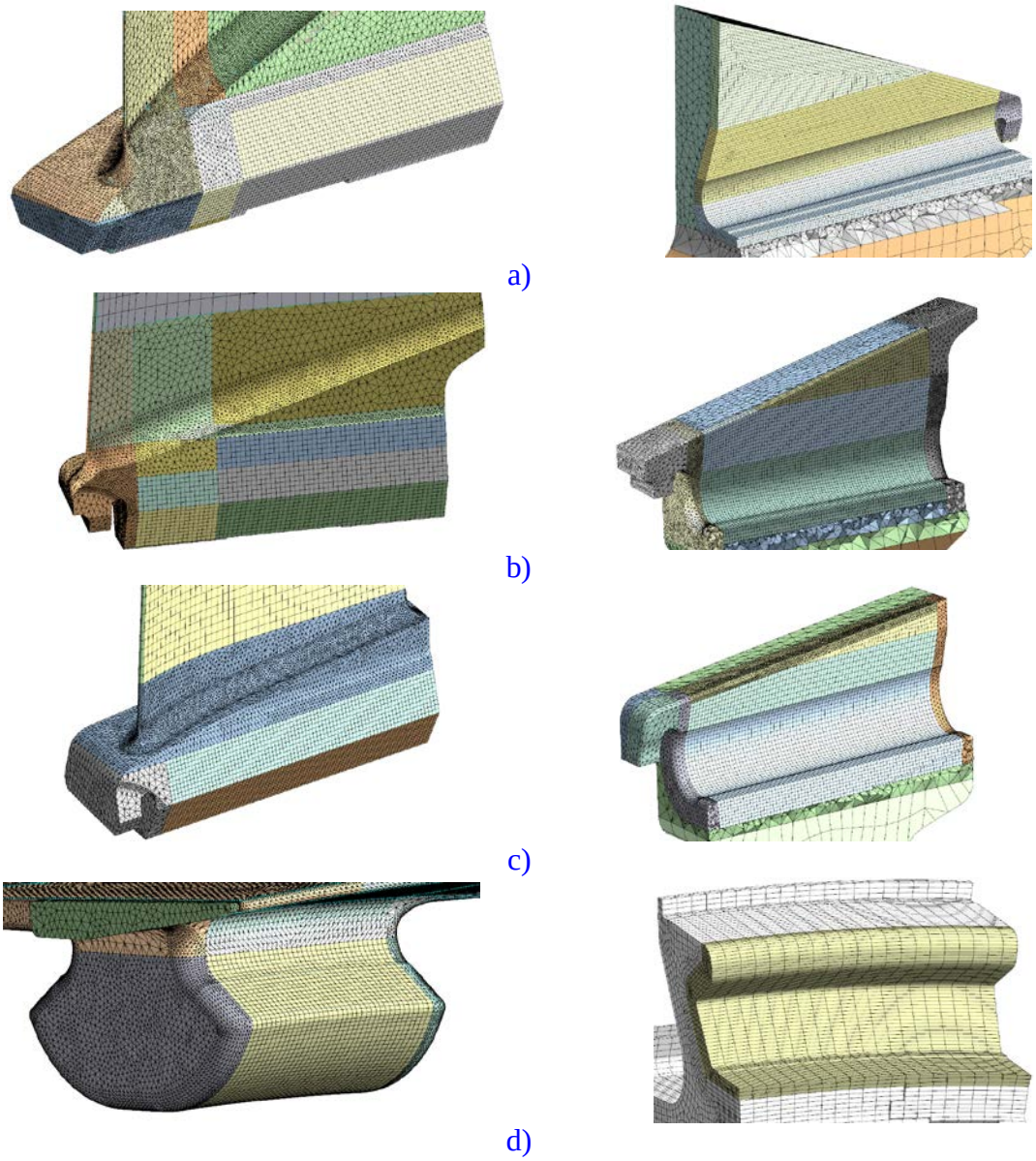

a) - RC of the first stage; b) - RC of the second stage; c) - RC of the third stage; d) - RC of the fourth stage

Figure 16: Grid quality for the locking joints of the blades

Table 2 shows the calculated total and radial displacements of the RC of the four stages. The analysis showed a significant change in the movements of the RC compressor. In general, there is a tendency to decrease the radial displacements and increase the circumferential ones (see Table 2).

The SSS analysis in the RC blades of 1 and 2 stages of the compressor showed a slight increase in the stress level compared to the original design (max 5%, see Table 3). For the remaining stages, there is a decrease in the stress level, and for the 3rd stage – an extremely sharp one (-47%), explained by the absence of the shroud in the optimized version of the blade.

Table 2: Comparison of the values of maximum displacements

No. of LPC stage	Displacements	Discrepancy (opt. relative to init.), %
1	Sum / Rad	+71.3 / -1.4
2	Sum / Rad	+25.2 / -9.7
3	Sum / Rad	-68.0 / -12.8
4	Sum / Rad	-91.4 / -22.7

Table 3: Comparison of the values of the maximum stresses in blade elements

No. of LPC stage	Stresses	Discrepancy, %
1	VM	+2.8**
	S1	+4.2**
2	VM	+3.4**
	S1	+4.7**
3	VM	-46.9*
	S1	-47.0*
4	VM	-10.7*
	S1	-6.0*

* – the colors indicate deviations (* - negative, ** - positive up to 10%, *** - positive more than 10%)

Table 4: Comparison of the values of the maximum stresses in blade lock elements

No. of LPC stage	Stresses	Discrepancy, %
1	VM	+27.3***
	S1	+19.6***
2	VM	-4.70*
	S1	-25.7*
3	VM	-21.3*
	S1	-22.0*
4	VM	-19.7*
	S1	-18.0*

* – the colors indicate deviations (* - negative, ** - positive up to 10%, *** - positive more than 10%)

Table 5: Comparison of the values of the maximum stresses in disk lock elements

No. of LPC stage	Stresses	Discrepancy, %
1	VM	-5.6*
	S1	-3.8*
2	VM	-0.5*
	S1	-2.4*
3	VM	-10.1*
	S1	-12.0*
4	VM	-5.7*
	S1	-16.0*

* – the colors indicate deviations (* - negative, ** - positive up to 10%, ** - positive more than 10%)

The SSS pattern in the blade and disc lock shows local stress spikes in the contact zone. The peak values of stresses in these areas are not indicative and should be attributed to the artifacts of

the FE analysis. The analysis of zones with a characteristic smooth and continuous distribution pattern shows a decrease in stresses compared to the initial geometry of the compressor RC for all stages, except for 1 RC, where an increase in the stress level in the blade lock by 27% is shown (see Tables 4 and 5).

The SSS analysis in RC disks also shows a moderate decrease in the stress level (from 3 to 9%) in the optimized design (see Table 6).

Table 6: Comparison of the values of the maximum stresses in disk elements

No. of LPC stage	Stresses	Discrepancy, %
1	VM	-6.79
	S1	-6.31
2	VM	-4.25
	S1	-3.89
3	VM	-7.02
	S1	-7.00
4	VM	-9.29
	S1	-9..85

* – the colors indicate deviations (* - negative, ** - positive up to 10%, *** - positive more than 10%)

Next, the dynamics were calculated for both the optimized and the initial design of the LPC RC, which FE models are similar in terms of geometry and boundary conditions to the models for strength described earlier. The order of the grid model is reduced to speed up the dynamic's calculations. All created contact pairs work as rigid linear contact (option bonded).

The calculation for the natural frequencies of the impellers was carried out in two versions – with an unloaded RC in normal atmospheric conditions and considering the SSS of the design when working in the design mode. The range in which the natural frequencies are searched is assigned based on the estimate of the maximum number of stator blades in the LPC and the rotation speed of the rotor in the operating mode. Thus, the range of finding the natural frequencies of the RC is limited to 14.5 kHz.

As a result of the calculation, the natural frequencies and corresponding oscillation forms of the RC are obtained in two design forms – optimized and non-optimized LPC.

According to the results of the comparative modal analysis, the following conclusions can be drawn:

- optimized blades of the RC of 1, 2, and 4 stages of the LPC showed an increase in the frequencies of the first 6 natural forms of vibrations;
- blades of the 3rd stage, due to the absence of the shroud in the optimized design, showed a decrease in the frequencies of the first 4 natural forms of vibrations;
- total number of resonant forms of vibrations of the optimized blades of 1, 2, and 3 stages is less than that of the original design;
- resonance of the 1st stage of the original RC (1 form 3 harmonic, see Figure 17) disappeared in the optimized design (see Figure 18).

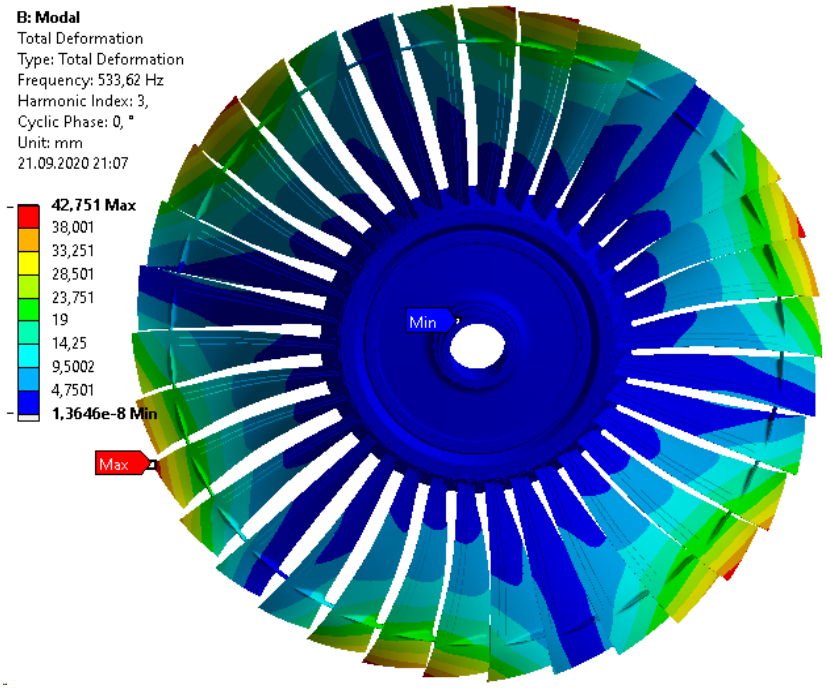

Figure 17: Resonant form-1 of the initial RC of the 1st stage of the LPC

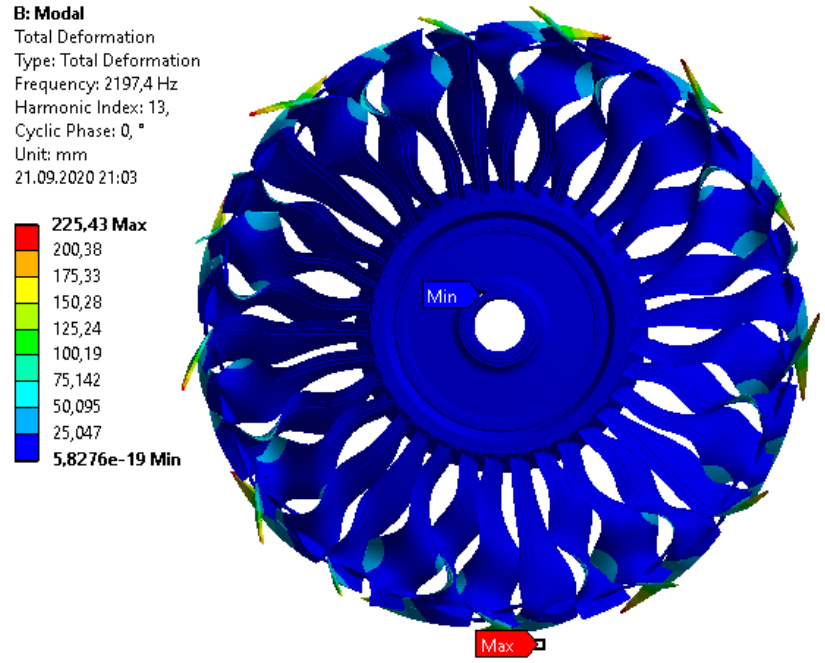

Figure 18: Resonant form-1 of the optimized RC of the 1st stage of the LPC

4 Conclusion

Based on the results of the work, the LPC was optimized, which provides an increase in the adiabatic efficiency of the compressor by $\Delta\eta^*_k$ = +2.57%, while meeting all requirements and limitations. The main results obtained in the course of the work:

According to the results of the primary optimization, an increase in the LPC efficiency was achieved by $\Delta\eta^*_k$ = +2.67%. Work has been carried out on preliminary SSS improvement of optimized blades RC1 and RC2 by compensating gas forces with centrifugal forces due to the displacement of the centers of mass of the blade cross-sections.

The calculation of the LPC characteristics on the pressure branches 0.8, 0.9, and 0.95 n was performed, where the efficiency of the developed LPC was confirmed on the branches 0.8 and 0.9 ($\Delta\eta^*_k$ = +2...4%), and insufficient air consumption was observed on the 0.95 branches.

An additional variant of an optimized LPC with locally enlarged peripherals has been developed, which fully meets the requirements for efficiency and performance in the entire operating range $\Delta\eta^*_k$ = +0.6...3.1%.

The static and dynamic analysis of the initial and final optimized LPC structures is carried out, the disappearance of the dangerous resonance of the RC of the 1st stage in the optimized design is shown.

5 Availability of Data and Material

Data can be made available by contacting the corresponding author.

6 Acknowledgement

This work was financially supported by the Ministry of Science and Higher Education of the Russian Federation in the framework of the Federal Program “Research and Development in Priority Directions for the Development of the Scientific and Technological Complex of Russia for 2014-2020”. Agreement on the provision of a grant in the form of subsidy No. 075-15-2019-1710 dated December 2, 2019 (internal number 05.608.21.0275). Unique identifier: RFMEFI60819X0275.

7 References

[1] Cumpsty NA. Compressor aerodynamics. Malabar: Krieger Publishing Company. 2004.

[2] Kato D, Pallot G, Sugihara A and Aotsuka M. Research and development of a high performance axial compressor. IHI Eng. Review. 2014; 47(1): 49-56.

[3] Yu X and Liu B. Research on three-dimensional blade designs in an ultra-highly loaded low-speed axial compressor stage: Design and numerical investigations. Adv. in Mech. Eng. 2016; 8(10): 1-16.

[4] Amoo LM. On the design and structural analysis of jet engine fan blade structures. Prog. in Aerosp. Sc. 2013; 60: 1-11.

[5] Zheng X and Li Zh. Blade-end treatment to improve the performance of axial compressors: An overview Prog. in Aerosp. Sc. 2017; 88: 1-14.

[6] Boyko AV, Govorushchenko YuN, Ershov SV, Rusanov AV, Severin SD. Aerodynamic calculation and optimal design of the flow part of turbomachines. Monograph - Kharkiv, KhPI, 2002; 356p.

[7] Egorov IN, Fedechkin KS, et al. Optimization of the gas turbine engine parts using methods of numerical simulation. ASME paper GT-2007-28205. 2007.

[8] Kato D, Pallot G, Sugihara A, Aotsuka M. Research and development of a high-performance axial compressor. IHI Eng. Review. 2014; 47(1): 49-56.

[9] Yu X and Liu B. Research on three-dimensional blade designs in an ultra-highly loaded low-speed axial compressor stage: Design and numerical investigations. Adv. in Mech. Eng. 2016; 8(10): 1-16.

[10] Burguburu S, Toussaint C, et al. Numerical Optimization of Turbomachinery Bladings. ASME paper GT-2004-22605. 2004.

[11] Baturin OV, Popov GM, Goryachkin ES, Smirnova YuD. Reprofiling a three-stage axial compressor using mathematical optimization methods. Proceedings of MAI. 2015; 82.

[12] Shabliy LS. Problems of optimization of multi-stage compressors in the creation of promising gas turbine engines. Bulletin of the Samara State Aerospace University. 2012; 3(34): 192-196.

[13] Matveev VN, Popov GM, Goryachkin ES. Optimization of the installation angles of the blade crowns of a multi-stage high-pressure compressor of the GTE. Proceedings of the Samara Scientific Center of the Russian Academy of Sciences. 2013; 6(4): 929-936.

[14] NUMECA. Numeca's Flow Integrated Environment for Turbomachinery and Internal Flows. User Manual, Numeca Int., Brussels, Belgium. 2008.

[15] ANSYS. Solver Theory Guide: ANSYS CFX documentation Release 17.2. ANSYS Inc., USA. 2016.

[16] Snegirev AYu. High-performance computing in technical physics. Numerical modeling of turbulent flows. 2009. St. Petersburg: Publishing House of the Polytechnic University.

[17] Piovesan T, Magrini A, Benini E. Accurate 2-D modelling of transonic compressor cascade aerodynamics Aerospace. 2019; 6(57). DOI: 10.3390/aerospace6050057

[18] Launder BE, Spalding DB. The numerical computation of turbulent flows, Computer Methods in Applied Mechanics and Engineering. 1974; 3(2): 269-289.

[19] Boussinesq, J. Theorie de l'Ecoulemen Tourbillant, Mem. Presentes par Divers Savants Acad. Sci. Inst. Fr. 1877; 23:46-50.

[20] Spalart, PR. Strategies for turbulence modelling and simulation. Intern. Journal of Heat and Fluid Flow. 2000; 21: 252-263.

Mikhail Leonidovich Zhivirikhin is an engineer at FGAOU Vo "SPbPU". His research interests are Gas Turbine Engines, Blades, Gas Dynamics, Parametric Optimization

Dr. Aleksey Sergeevich Tikhonov is a Leading Researcher of the Federal State Autonomous Educational Institution of Higher Education "SPbPU". He is a Candidate of Technical Sciences. His research interests are Gas Turbine Engines, Gas Dynamics, Engineering Software Development.